JOURNAL OF AIRCRAFT
Vol. 35, No. 1, January–February 1998

Active Suppression of Aircraft Panel Vibration with Piezoceramic Strain Actuators

Jonathan D'Cruz*
Defence Science and Technology Organisation, Melbourne, Victoria 3001, Australia

The out-of-plane vibration of a panel on an aircraft tailplane, excited by random noise in the 100–500 Hz range, was suppressed by an active controller that used four piezoceramic patches, two as strain actuators and two as strain sensors. The strain energy levels at these sensor locations were significantly reduced. Three accelerometers at arbitrarily chosen locations elsewhere on the panel demonstrated that the out-of-plane vibrational energy levels were also reduced there. The multi-input, multi-output digital controller, designed by a physically meaningful technique, also resulted in a system with good robustness properties.

Introduction

IN the interests of increased performance and efficiency, aircraft structures contain thin panels with relatively few supports. Because of this, these panels are prone to vibrate at excessive amplitudes. In view of the low cost of computing power, digital controllers, implemented with suitable actuators and sensors, are an attractive proposition as a means by which these vibrations may be actively suppressed. The readily available piezoceramic strain actuator is compact and lightweight and does not need a support structure for reaction purposes. Therefore, digital controllers, implemented via piezoceramic strain actuators, are a seemingly ideal solution to such panel vibration problems.

Over the past decade, there have been numerous studies in the field of active vibration suppression with piezoelectric strain actuators. Beams[1–5] have often been the subject of these studies, as have plates and shells.[6–11]

More recently, the concepts thus developed have been applied to more complex problems, many of these applications being aeronautical. The problems examined include the control of panel flutter,[12,13] as well as rotary[14] and fixed-wing[15–18] aeroelastic responses with strain actuation. Weisshaar[19] provides an extensive survey of the research that has taken place in the field, with an emphasis on fixed-wing and shell structures. It is pointed out there that more experiments need to be conducted to verify the concept of aeroelastic control with strain actuation.

To address the relative scarcity of research programs that demonstrate active control via strain actuation on actual aircraft structures, the study reported in this paper was initiated. In this study, one of the panels on the fin of a CT-4 (an aircraft previously used by the Royal Australian Air Force as a basic trainer) was excited by random noise with a bandwidth of 100–500 Hz. Several modes were excited as a result, and suitable locations were determined for the attachment of two lead zirconate titanate (PZT) piezoceramic strain sensors and strain actuators to control these modes.

A two-input, two-output digital feedback controller with direct feedthrough was then designed and implemented, with the result that the vibration levels were significantly attenuated. Three accelerometers were attached to the panel at arbitrarily chosen points to ensure that the attenuation was not confined to the locations of the two PZT strain-feedback sensors; the accelerometers confirmed this. Furthermore, the control design technique was a physically meaningful one that resulted in a system with good robustness properties.

It should be noted that the purpose of this paper is not to provide a new technique of controller design; rather, it is to provide an insight into the application of digital feedback control with piezoelectric strain actuators and sensors to an actual aircraft structure.

Experimental Setup

Figure 1 shows the fin suspended horizontally by three soft springs. Random-force input was provided by an electromagnetic shaker attached to the lower surface at a web–spar junction. Four PZT patches and three accelerometers may be seen in Fig. 1. Figure 2 is a schematic of the closed-loop system with the external noise source. The digital control law was implemented by a 133-MHz Pentium personal computer.

The four PZT patches, each $1.25 \times 1.5 \times 0.0075$ in., were adhesively bonded to the fin panel. The patches consisted of a layer of PZT, with nickel electrodes on the top and bottom surfaces. Electrical contact was established via silver-loaded epoxy between the lower PZT electrode and the metal fin structure, which then provided the earth–return path.

Determination of Suitable Sensor and Actuator Locations

The locations of the sensors and actuators are dependent on the modes being controlled. For an isotropic structure, the sensors and actuators respond and impart a quantity proportional to the sum of principal strains, i.e., the bulk strain. The structure under test is assumed to be thin-walled, with zero through-the-thickness stresses or strains. Therefore, the bulk strain is proportional to the curvature. It is therefore important to attach the actuators and sensors at points where these quantities are nonzero, and preferably where they are at a maximum.

However, it is a difficult task to obtain a full-field measure of the bulk strain. (A thermoelastic technique[20] would, in theory, yield such a measure, but the strain levels involved here were deemed too low for such a technique to be usable in practice.) It was therefore proposed that the bulk-strain distribution be inferred from visualizations of the displacement mode shapes.

Figure 3 shows the power spectra of the three accelerometer signals when the panel was excited by the shaker with random

Received June 16, 1996; revision received July 31, 1997; accepted for publication Aug. 11, 1997.

*Research Scientist, Airframes and Engines Division, Aeronautical and Maritime Research Laboratory; currently Senior Specialist Engineer, General Motors–Holden's Automotive Ltd., MP 305, Noise and Vibration Group, Salmon Street, Port Melbourne, Victoria 3207, Australia. Member AIAA.

a)

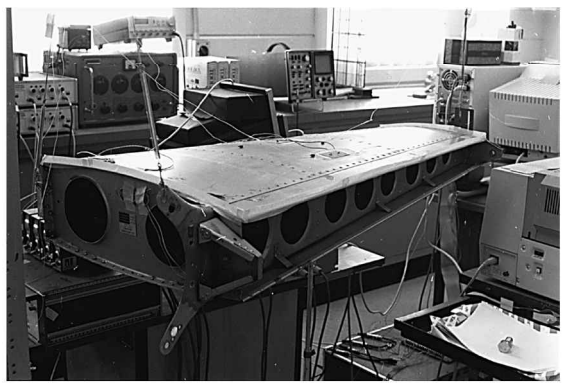

b)

Fig. 1 Experimental apparatus: a) view of fin with shaker from outboard top, and b) view of fin from inboard trailing edge.

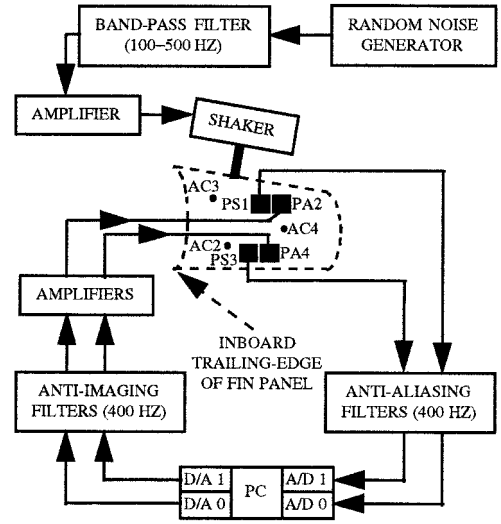

Fig. 2 Closed-loop system with external noise source (AC = accelerometer, PS/A = PZT sensor/actuator).

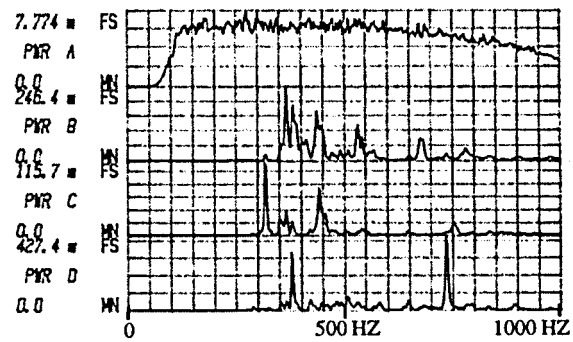

Fig. 3 Power spectra (A = shaker amplifier input; B, C, D = AC2, 3, 4).

noise in the 100–1000 Hz range, the accelerometer positions having been arbitrarily chosen. The first four dominant modes have frequencies of approximately 320, 370, 380, and 440 Hz. The panel was consequently excited sinusoidally at these frequencies in turn (with a small degree of modal tuning), to obtain the nodal-line patterns appearing in Fig. 4.

To provide a guide by which the bulk strain distributions may be inferred from the modal displacement patterns, a dynamic finite element analysis was conducted on a panel of nominally similar configuration. For the purposes of this analysis, the edges of the panel were assumed to be clamped, with the two chordwise edges being of constant curvature. Also, structural damping was taken to be zero in view of the light damping present in the actual structure. Figure 5 shows one of the modal patterns obtained, and Fig. 6 the corresponding bulk-strain field. Four hundred four-node plate elements (20 chordwise and 20 spanwise) were used for the finite element model.

To accurately predict the complicated, high-frequency modes of the panel, such as those illustrated in Fig. 4, it will be necessary to, at a minimum, 1) accurately represent the riveted-edge panel boundaries; 2) obtain the appropriate edge curvatures; and 3) model more of the structure, including adjacent panels, ribs, spars, stringers, etc. This is a task of significant difficulty. Nevertheless, in view of the assumptions made, the displacement modal frequency and pattern of Fig. 5 were not unlike those illustrated in Fig. 4.

From Figs. 5 and 6, it may be seen that, away from the edges, the displacement and bulk-strain fields had local extrema at very similar points on the panel. This fact was used to infer the distribution of the actual bulk-strain fields from the displacement nodal-line patterns of Fig. 4. Figure 7 shows the thus-deduced locations, where the bulk strain was expected to be a (local) maximum or minimum, and the locations consequently chosen for the PZT sensors and actuators.

With the actuators and sensors on the panel as shown in Fig. 7, a 100–500-Hz random signal was sent to the shaker. The power spectra of the resulting three accelerometer and two PZT sensor signals appear in Figs. 8 and 9. An examination of Fig. 8 (in relation to the 0–500-Hz portion of Fig. 3) reveals that the attachment of the PZT sensors and actuators did not significantly alter the spectral content of the accelerometer signals.

According to the preceding argument, PS1 should have been sensitive to the 366.7- and 445.5-Hz modes, with PS3 responding to the 317.8-, 377.2-, and, to a smaller extent, 445.5-Hz modes. (The slight differences in these frequencies from 320, 370, 380, and 440 Hz may be attributable to the attachment of the PZT patches to the structure.) As may be seen from Fig. 9, PS1 did respond to the 366.7-Hz mode, whereas PS3 registered strong 317.8- and 377.2-Hz components in its response. The 445.5-Hz mode, although excited by the shaker [see the power spectral density (PSD) plot for AC2 in Fig. 8], did not appear to be present to any great extent in the signal from either PS1 or PS3. A possible reason for this is that the 445.5-Hz mode, with its higher density of nodal lines, was less tolerant to any mislocation of the strain sensors. A solution to this is to more accurately determine the whole-field modal displacements (and hence the bulk strain distribution), for instance with a scanning laser–Doppler vibrometer.

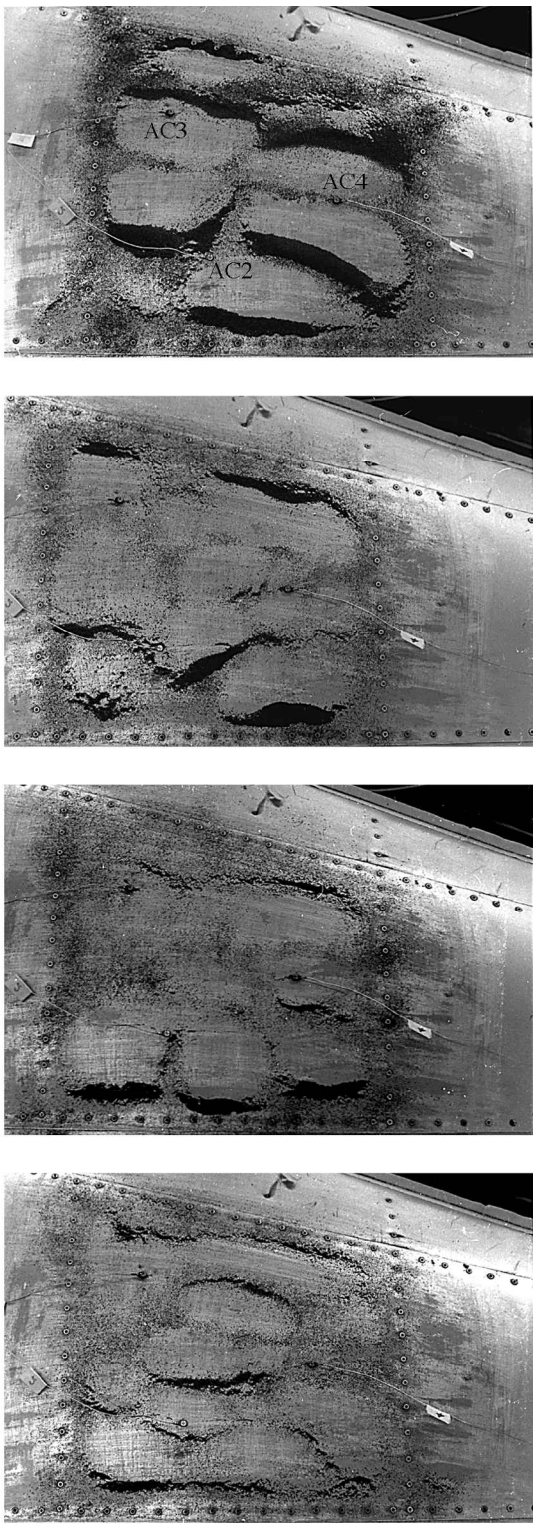

Fig. 4 Visualization of nodal lines (dark areas) for various modes. a) 317.8, b) 366.7, c) 377.2, and d) 445.5 Hz.

In view of the preceding discussion, it was decided that no attempt would be made to control the 445.5-Hz mode. The antialiasing and anti-imaging filters were therefore set to 400 Hz.

System Identification and Controller Design

The technique used to identify the system and to design the controller was based on that detailed by D'Cruz.[21] Briefly, the two-input, two-output system was decoupled into two single-input, single-output loops, one contained within the other. Such an approach is mathematically less complex and physically more intuitive than a full multivariable design. Nevertheless, as will be seen from the analysis of the system properties later in this paper, the closed-loop system that resulted also had good robustness properties.

Each set of adjacent PZT patches acted as the sensor and actuator for one of the single-input, single-output loops. PS1 and PA2 were the sensor and actuator for the inner loop, with PS3 and PA4 serving the same purpose for the outer loop. In

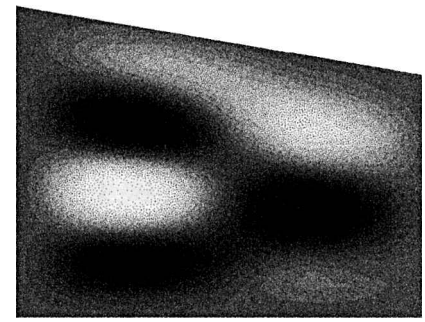

Fig. 5 FEA displacement modal pattern at 349.3 Hz (white = maximum, black = minimum).

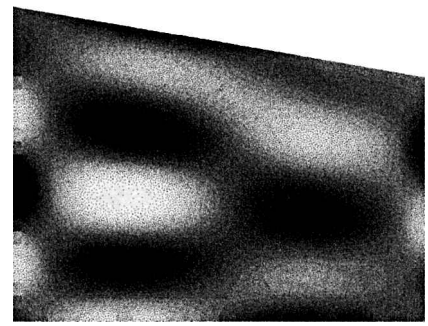

Fig. 6 FEA bulk-strain modal pattern at 349.3 Hz (white = maximum, black = minimum).

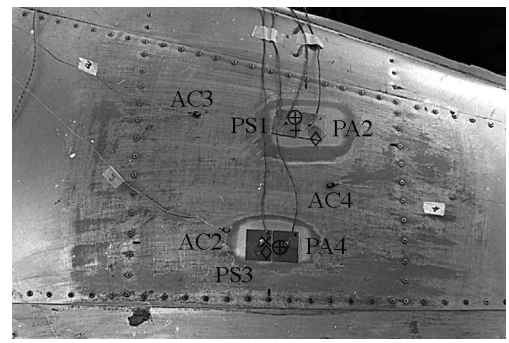

Fig. 7 Panel with sensors and actuators (×, +, ◇, ⊕ = 317.8-, 366.7-, 377.2-, and 445.5-Hz mode local displacement extrema).

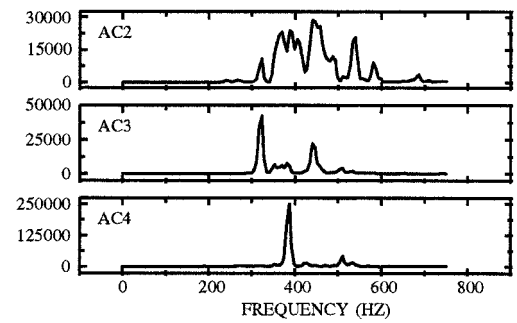

Fig. 8 Power spectra of accelerometer signals for 100–500-Hz shaker excitation.

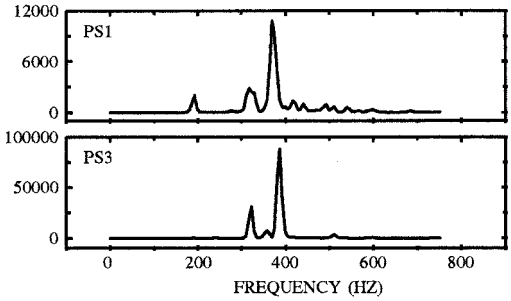

Fig. 9 Power spectra of PZT sensor signals for 100–500-Hz shaker excitation.

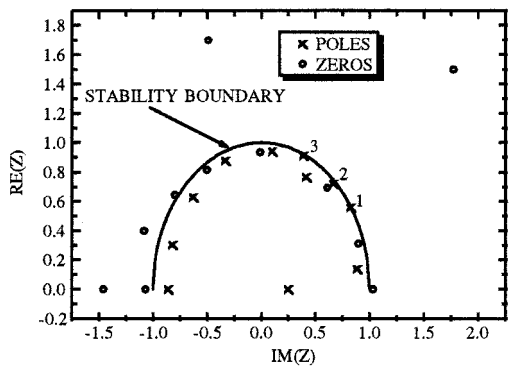

Fig. 10 Poles and zeros for inner loop (discrete time representation).

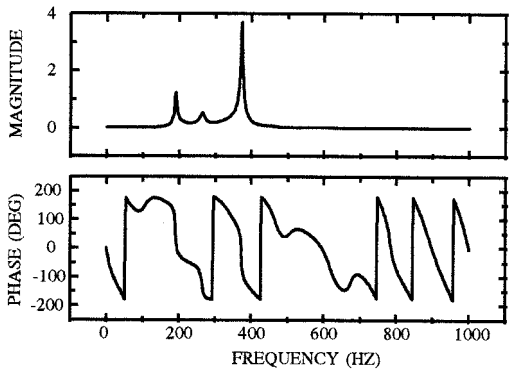

Fig. 11 Continuous time transfer function for inner loop.

view of the frequencies of the modes being controlled, the sampling rate selected was 2000 Hz.

The inner loop was first identified by exciting the panel via PA1 with known random noise and measuring the response of PS2. Figure 10 shows, in the discrete time domain, the poles and zeros for this loop, with Fig. 11 being the continuous time representation of the transfer function (based on the model variance, a 20th-order representation was used). There were three lightly damped poles with the following frequencies: 1) pole 1: f = 191.0 Hz, 2) pole 2: f = 264.9 Hz, and 3) pole 3: f = 373.1 Hz. An examination of Figs. 8 and 9 reveals that there were panel response components close to the frequencies of poles 1 and 3. (A reason for the discrepancy is that a transfer function is now being considered.) It was therefore concluded that only these two poles would be moved in the process of the inner-loop pole placement procedure.

To restrict the number of possibilities under consideration, it was decided that only the damping factor of the poles would be varied (increased). The damping factor is given by $\alpha = (\ell n\ R)/T$, where R is the distance of the pole from the origin, and T is the intersample time. Additionally, the relative amounts by which each pole was moved were such that the

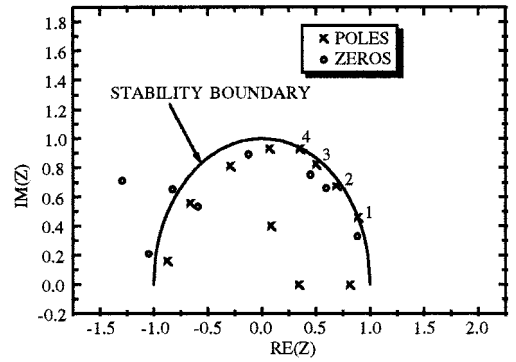

Fig. 12 Poles and zeros for outer loop (discrete time representation; zeros at z = 7.92 and 1.17 + 2.93i not plotted).

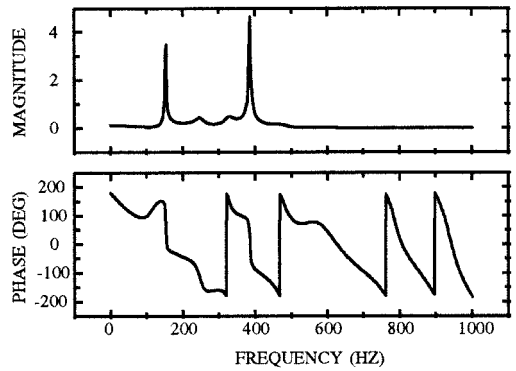

Fig. 13 Continuous time transfer function for outer loop.

control energy per unit increase in damping factor (with the other pole in its open-loop position) was the same for both poles. With this strategy, the closed-loop pole positions for the inner loop finally settled upon were such that the damping factors increased to 5.50 times the open-loop value for pole 1, and 5.11 times the open-loop value for pole 3.

With this inner-loop controller operating, the outer loop was identified by feeding a known random signal to PA4 and capturing the response of the panel as measured by PS3. Discrete and continuous time representations of the outer loop with the closed inner loop appear in Figs. 12 and 13, respectively. A 20th-order model was again found to have a sufficiently small variance when compared to the mean square sensor signal and was therefore again used. The frequencies of the four lightly damped poles of Fig. 12 are 1) pole 1: f = 153.1 Hz, 2) pole 2: f = 248.0 Hz, 3) pole 3: f = 327.6 Hz, and 4) pole 4: f = 386.5 Hz. If these frequencies are examined in relation to Figs. 8 and 9, it will be seen that the panel responded to the 100–500-Hz shaker excitation at frequencies close to those of poles 3 and 4. (An additional reason for the discrepancy here is that there was a closed loop in operation when the poles were determined.) Although there was an insignificant level of response at pole 1, it is desirable to increase its level of damping to avoid exciting that mode. Hence, the outer-loop controller was designed by increasing the damping of poles 1, 3, and 4.

The methodology adopted to limit the number of possibilities for the outer-loop controller was identical to that used for the inner-loop controller design, i.e., only damping was varied, with the control energy per damping-factor unit increase the same for each pole (with all other poles in their original open-loop positions). The outer-loop controller settled upon had 25.00, 1.47, and 6.05 as the respective ratios of the prescribed damping factors of poles 1, 3, and 4 to the original damping factors.

Closed-Loop System Behavior

The open-loop and closed-loop systems may be compared by examining the power spectra of the three accelerometer and

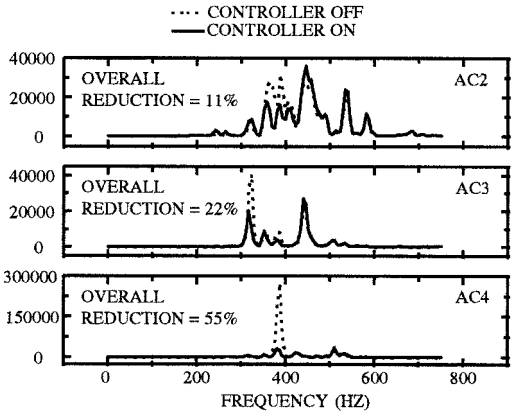

Fig. 14 Power spectra of unfiltered accelerometer signals.

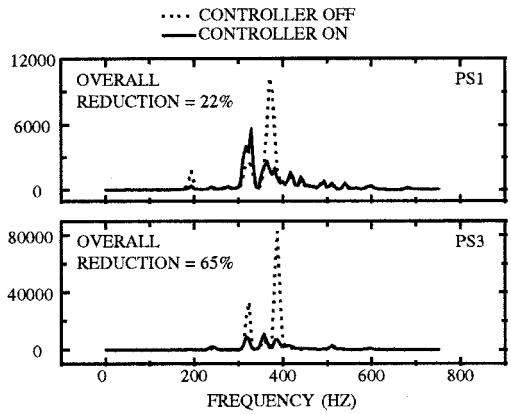

Fig. 15 Power spectra of unfiltered PZT sensor signals.

two PZT sensor signals without and with the two-input, two-output controller in operation. Figures 14 and 15 provide such a comparison.

It is evident from Fig. 14 that the controller reduced the overall vibrational energy at each of the three accelerometer locations. There is a relatively small increase in the response at about 440 Hz for both AC2 and AC3. A possible cause of this is that the shape of the 440-Hz mode was altered in such a manner by the controller as to place AC2 and AC3 at locations where the contribution from this mode to the acceleration response was higher. Another possibility is that a small amount of spillover is occurring. Nevertheless, the overall (acceleration) vibrational energy seen by AC2 and AC3 was significantly reduced.

Figure 15 shows that the controller again significantly reduced the overall (strain) vibrational energy at both PS1 and PS3, in spite of a slight increase at the former location of the response at approximately 320 Hz.

Robustness Properties

It is important that the controller be able to cope with variations in the system characteristics. A controller that can do this well is termed robust. Two measures of robustness (or, more specifically, relative stability) are the gain margin and the phase margin. The former is a measure of how much the gain of a system can increase before the onset of instability, and the latter is a measure of the amount of additional phase-lag that can be tolerated before instability results.[22]

The gain and phase margins, G_M and ϕ_M, were computed for each single-input, single-output loop. For the inner loop, $G_M = -9.5$ dB and $\phi_M = -74$ deg. For the outer loop, $G_M = 10.4$ dB and $\phi_M = 73$ deg. As these values were significantly different from 0 dB and 0 deg, both control loops may be seen to have good robustness properties.

Conclusions

A technique for actively suppressing the random vibrations of an aircraft panel has been presented. This included a method for selecting suitable locations for sensors and actuators and a physically intuitive means for designing the digital controller. What resulted was a system that produced significant reductions in the vibrational energy at the locations of the feedback sensors as well as at other arbitrarily chosen locations. Furthermore, the system had good robustness properties.

Possible improvements to the previously described technique include 1) obtaining a more accurate measure of the whole-field modal displacements and, consequently, the modal bulk-strain distributions, hence improving the accuracy of the suggested sensor and actuator locations; 2) increasing the number of sensors (a technique for achieving this that uses a physically meaningful linear design technique for the controller is described by D'Cruz[23]); 3) weighting the pole movements so that the relative levels of response at particular frequencies are taken into account; and 4) configuring the PZT patches so that genuine sensor–actuator colocation is attained. The benefits that may be obtained by more accurately modeling the structure are probably unjustified in view of the high level of complexity a model would need to have to properly predict the high-density modes being controlled.

Acknowledgements

The author is grateful to A. Barylko for writing the drivers for the cards that implemented the digital controller, and to P. A. Farrell and T. G. Ryall for their helpful suggestions.

References

[1]Bailey, T., and Hubbard, J. E., Jr., "Distributed Piezoelectric-Polymer Active Vibration Control of a Cantilever Beam," *Journal of Guidance, Control, and Dynamics*, Vol. 8, No. 5, 1985, pp. 605–611.

[2]Crawley, E. F., and De Luis, J., "Use of Piezoelectric Actuators as Elements of Intelligent Structures," *AIAA Journal*, Vol. 25, No. 10, 1987, pp. 1373–1385.

[3]Burke, S. E., and Hubbard, J. E., Jr., "Distributed Actuator Control Design for Flexible Beams," *Automatica*, Vol. 24, No. 5, 1988, pp. 619–627.

[4]Song, O., Librescu, L., and Rogers, C. A., "Adaptive Response Control of Cantilevered Thin-Walled Beams Carrying Heavy Concentrated Masses," *Journal of Intelligent Material Systems and Structures*, Vol. 5, No. 1, 1994, pp. 42–48.

[5]Anderson, E. H., and Hagood, N. W., "Simultaneous Piezoelectric Sensing/Actuation: Analysis and Application to Controlled Structures," *Journal of Sound and Vibration*, Vol. 174, No. 5, 1994, pp. 617–639.

[6]Crawley, E. F., and Lazarus, K. B., "Induced Strain Actuation of Isotropic and Anisotropic Plates," *AIAA Journal*, Vol. 29, No. 6, 1991, pp. 944–951.

[7]Tzou, H. S., and Fu, H. Q., "A Study of Segmentation of Distributed Piezoelectric Sensors and Actuators, Part I: Theoretical Analysis," *Journal of Sound and Vibration*, Vol. 172, No. 2, 1994, pp. 247–259.

[8]Tzou, H. S., and Fu, H. Q., "A Study of Segmentation of Distributed Piezoelectric Sensors and Actuators, Part II: Parametric Study and Active Vibration Controls," *Journal of Sound and Vibration*, Vol. 172, No. 2, 1994, pp. 261–275.

[9]Falangas, E. T., Dworak, J. A., and Koshigoe, S., "Controlling Plate Vibrations Using Piezoelectric Actuators," *IEEE Control Systems*, Vol. 14, No. 4, 1994, pp. 34–41.

[10]Clark, R. L., and Fuller, C. R., "Active Control of Structurally Radiated Sound from an Enclosed Finite Cylinder," *Journal of Intelligent Material Systems and Structures*, Vol. 5, No. 3, 1994, pp. 379–391.

[11]Ghidella, J. R., "Simulation and Control of Flexible Structures," Ph.D. Dissertation, Dept. of Aeronautical Engineering, Univ. of Sydney, Sydney, Australia, 1995.

[12]Scott, R. C., and Weisshaar, T. A., "Panel Flutter Suppression Using Adaptive Material Actuators," *Journal of Aircraft*, Vol. 31, No. 1, 1994, pp. 213–222.

[13]Lai, Z., Xue, D. Y., Huang, J.-K., and Mei, C., "Panel Flutter Limit-Cycle Suppression with Piezoelectric Actuation," *Journal of Intelligent Material Systems and Structures*, Vol. 6, No. 3, 1995, pp. 274–282.

[14]Nitzsche, F., and Brietbach, E. J., "Using Adaptive Structures to Attenuate Rotary Wing Aeroelastic Response," *Journal of Aircraft*, Vol. 31, No. 5, 1994, pp. 1178–1188.

[15]Barrett, R., "Active Plate and Wing Research Using EDAP Elements," *Journal of Smart Materials and Structures*, Vol. 1, No. 3, 1992, pp. 214–226.

[16]Reich, G. W., Van Schoor, M. C., Lin, C. Y., and Crawley, E. F., "An Active Aeroelastic Wing Model for Vibration and Flutter Suppression," AIAA Paper 95-1193, April 1995.

[17]McGowan, A.-M. R., Heeg, J., and Lake, R. C., "Results of Wind-Tunnel Testing from the Piezoelectric Aeroelastic Response Tailoring Investigation," AIAA Paper 96-1511, April 1996.

[18]Librescu, L., Meirovitch, L., and Song, O., "Integrated Structural Tailoring and Control Using Adaptive Materials for Advanced Aircraft Wings," *Journal of Aircraft*, Vol. 33, No. 1, 1996, pp. 203–213.

[19]Weisshaar, T. A., "Aeroservoelastic Control with Active Materials — Progress and Promise," *Proceedings of the International Forum on Aeroelasticity and Structural Dynamics*, Royal Aeronautical Society, London, 1995, pp. 6.1–6.13.

[20]Ryall, T. G., and Wong, A. K., "Design of a Focal-Plane Array Thermographic System for Stress Analysis," *Experimental Mechanics*, Vol. 35, No. 2, 1995, pp. 144–147.

[21]D'Cruz, J., "Global Multivariable Vibration Control with Distributed Piezoceramic Actuators," *Journal of Intelligent Material Systems and Structures*, Vol. 6, No. 3, 1995, pp. 419–429.

[22]Franklin, G. F., Powell, J. D., and Workman, M. L., *Digital Control of Dynamic Systems*, 2nd ed., Addison–Wesley, Reading, MA, 1990, p. 201.

[23]D'Cruz, J., "Global Attenuation of Random Vibrations in a Tapered and Swept Panel," *Journal of Sound and Vibration*, Vol. 199, No. 5, 1997, pp. 751–776.